

Pinwheel-Shaped Heterobimetallic Lanthanide Alkali Metal Binaphtholates: Ionic Size Matters!

Helen C. Aspinall,* Jamie F. Bickley, Jennifer L. M. Dwyer, Nicholas Greeves, Richard V. Kelly, and Alexander Steiner

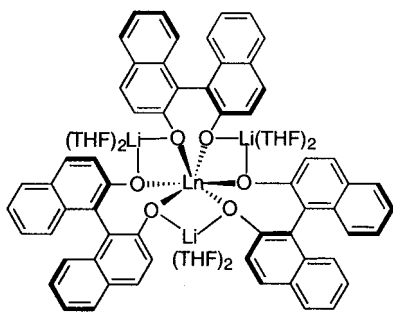
Donnan and Robert Robinson Laboratories, Department of Chemistry,
University of Liverpool, Crown Street, Liverpool, L69 7ZD, U.K.

Received July 18, 2000

Anhydrous alkali metal lanthanide binaphtholates $M_3[Ln(binol)_3]$ ($M = Li, Na$; $Ln =$ lanthanide or yttrium; $H_2binol =$ binaphthol) are prepared by reaction of $[Ln\{N(SiMe_3)_2\}_3]$ with 3 equiv of $MHbinol$. Reaction of $[Ln\{N(SiMe_3)_2\}_3]$ ($Ln = Y$ or Yb) with 3 equiv of *rac*- $LiHbinol$ gives a racemic mixture of *RRS*- and *SSR*- $Li_3[Ln(binol)_3]$ **2** as the only product. In contrast, reaction of $[Ln\{N(SiMe_3)_2\}_3]$ with 3 equiv of *rac*- $NaHbinol$ gives a racemic mixture of *RRR*- and *SSS*- $Na_3[Ln(binol)_3]$ when $Ln = Y$. When $Ln = Yb$, a 3:1 mixture of *RRR*-/*SSS*- and *RRS*-/*SSR*- $Na_3[Ln(binol)_3]$ is formed. Complexes have been characterized in solution by NMR spectroscopy. The 3-proton of the unique binol ligand in *RRS*- and *SSR*- $Li_3[Y(binol)_3]$ is shifted upfield by interaction with the π -system of a neighboring naphthyl ring. Analysis of paramagnetically induced 1H NMR shifts of Yb complexes shows them to be entirely dipolar in origin. X-ray crystal structures have been determined for the following compounds: *rac*- $[Li(THF)_2]_3[Y(binol)_3] \cdot THF$, **2a**; *rac*- $[Na(THF)_2]_3[Y(binol)_3]$, **3**; $[Li(OEt_2)]_3[Eu(S-binol)_3] \cdot [Li(OEt_2)]_3[Eu(S-binol)_3(H_2O)] \cdot 2Et_2O$, **4**; $[Li(THF)_2]_2[Li(OEt_2)][Yb(S-binol)_3] \cdot THF$, **5**; $[Na(THF)_2]_3[Yb(S-binol)_3]$, **6**; $[Na(THF)_2]_3[La(S-binol)_3(H_2O)]$, **7**.

Introduction

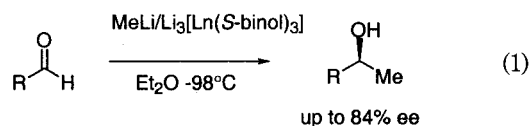
Heterometallic alkali metal lanthanide binaphtholates of general formula $M_3[Ln(binol)_3(H_2O)]$ first appeared in the early 1990s when Shibasaki showed them to be excellent enantioselective catalysts for a wide range of synthetically important reactions.^{1,2} We recently reported the synthesis of *anhydrous* analogues of Shibasaki's catalysts such as $[Li(THF)_2]_3[Ln(R-binol)_3]$ (**1**, $H_2binol =$ binaphthol; $Ln =$ lanthanide or yttrium).³



1

We demonstrated that when $M = Li$ and $Ln = La$, these complexes were highly effective reagents for enantioselective alkyl addition to aldehydes (reaction

1). Enantioselectivity decreased dramatically on changing the radius of Ln^{3+} from large (La) to small (Yb).



Shibasaki's work has shown that a specific combination of Ln and M is often best for a particular reaction. For example the hydrophosphonylation of acyclic imines proceeds with the highest ee when $Ln = La$ and $M = K$.⁴ In contrast, the highest ee's for cyclic imines are found with $Ln = Yb$ and $M = K$.⁵ The marked effect of the alkali metal is illustrated by the nitroaldol reaction, which is catalyzed with 94% ee when $M = Li$ and 2% ee when $M = Na$. The Michael addition shows a reversal of this observation: 92% ee is obtained when $M = Na$ and 2% when $M = Li$.¹ Our work on alkylation reactions would obviously be incompatible with the presence of acidic coordinated H_2O , and we have therefore always worked with anhydrous complexes. Shibasaki has generally worked with aquo complexes, although a recent paper has investigated the effect of H_2O (and base) on the catalysis of the aldol reaction.⁶

In view of the great sensitivity of reaction outcome to the identity of M and Ln , detailed structural study of a range of $M_3[Ln(binol)_3]$ complexes is of interest.

(1) Shibasaki, M.; Sasai, H.; Arai, T.; Iida, T. *Pure Appl. Chem.* **1998**, *70*, 1027–1034.

(2) Shibasaki, M.; Sasai, H.; Arai, T. *Angew. Chem., Int. Ed. Engl.* **1997**, *36*, 1237–1256.

(3) Aspinall, H. C.; Dwyer, J. L. M.; Greeves, N.; Steiner, A. *Organometallics* **1999**, *18*, 1366–1368.

(4) Sasai, H.; Arai, S.; Tahara, Y.; Shibasaki, M. *J. Org. Chem.* **1995**, *60*, 6656–6657.

(5) Groger, H.; Saida, Y.; Sasai, H.; Yamaguchi, K.; Martens, J.; Shibasaki, M. *J. Am. Chem. Soc.* **1998**, *120*, 3089–3103.

(6) Yoshikawa, N.; Yamada, Y. M. A.; Das, J.; Sasai, H.; Shibasaki, M. *J. Am. Chem. Soc.* **1999**, *121*, 4168–4178.

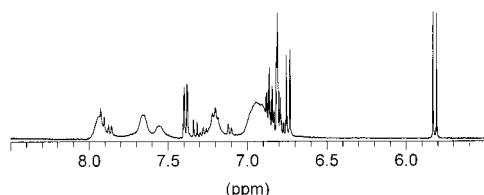


Figure 1. ^1H NMR spectrum (aromatic region) of *rac*-[Li(THF) $_2$] $_3$ [Y(binol) $_3$], **2a**.

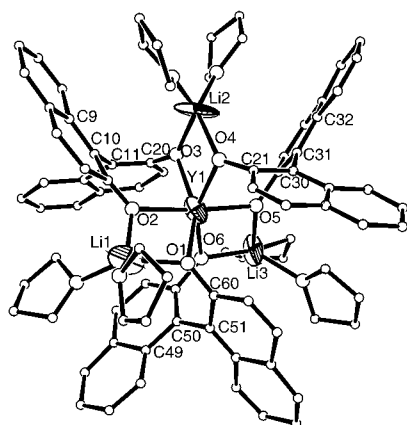
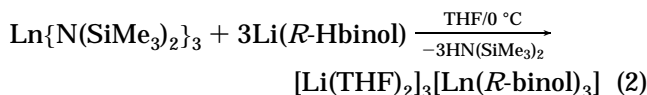


Figure 2. Molecular structure of [Li(THF) $_2$] $_3$ [Y(*R*-binol) $_2$ (*S*-binol)], **2a**.

Shibasaki has reported the structures of [Na(THF) $_2$] $_3$ [Ln(binol) $_3$ (H $_2$ O)] for the early lanthanides Ln = La, Pr, and Eu,^{7–8} and a preliminary structure (not fully refined) of [Li(THF) $_2$] $_3$ [Sm(binol) $_3$ (H $_2$ O)] has also been reported.⁹ However, there are as yet no structures reported for later Ln. In this paper we report the synthesis and structures of $\text{M}_3[\text{Ln}(\text{binol})_3]$ for a series of complexes including those of later lanthanides. We also report some investigations using racemic binaphthol.

Results and Discussion

Preparation of Anhydrous $\text{M}_3[\text{Ln}(\text{binol})_3]$. We have developed a straightforward synthesis of anhydrous $\text{M}_3[\text{Ln}(\text{binol})_3]$ starting from lanthanide trisilylamides [Ln{N(SiMe $_3$) $_2$] $_3$, which are extremely reactive with protic reagents. Addition of 3 equiv of the appropriate MHbinol (M = Li or Na) to [Ln{N(SiMe $_3$) $_2$] $_3$ gives $\text{M}_3[\text{Ln}(\text{binol})_3]$ cleanly and quantitatively as shown in reaction 2. The only byproduct is HN(SiMe $_3$) $_2$, which is volatile and easily removed in vacuo. Product can be isolated as a microcrystalline solid from THF–petroleum ether. The absence of $\nu(\text{OH})$ in the IR spectra of materials prepared in this way showed them to be anhydrous.



$\text{M}_3[\text{Ln}(\text{binol})_3]$ Complexes Prepared from *rac*-Binaphthol: A Remarkable Dependence on M. In the early days of this investigation, we used racemic

Table 1. Selected Bond Distances (Å) and Angles (deg) for **2**, **3**, **4**, **5**, and **6**

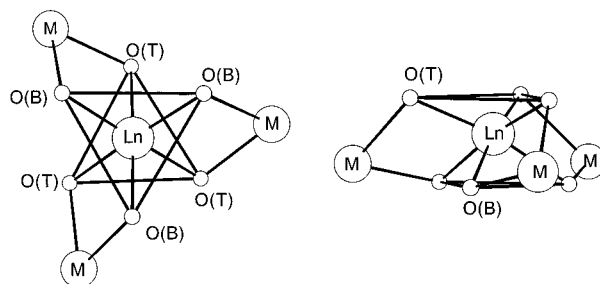
<i>RRS</i> -[Li(THF) $_2$] $_3$ [Y(binol) $_3$], 2a			
Y1–O1	2.224(10)	O1–Y1–O6	81.1(4)
Y1–O2	2.205(11)	O2–Y2–O3	82.6(4)
Y1–O3	2.256(9)	O4–Y1–O5	82.6(3)
Y1–O4	2.220(9)	O1–Li2–O2	81.9(13)
Y1–O5	2.220(9)	O3–Li2–O4	84.1(10)
Y1–O6	2.247(10)	O5–Li3–O6	87.8(10)
Li1–O1	2.04(3)	C9–C10–C11–C20	112.9(18)
Li1–O2	1.94(3)	C21–C30–C31–C32	108.8(16)
Li2–O3	2.00(3)	C60–C51–C50–C49	–120.6(17)
Li2–O4	2.13(3)		
Li3–O5	1.94(3)		
Li3–O6	1.88(3)		
[Na(THF) $_2$] $_3$ [Y(<i>R</i> -binol) $_3$], 3			
Y1–O1	2.227(6)	O1–Y1–O2	81.8(2)
Y1–O2	2.249(6)	O1–Y1–O22	79.7(2)
Na1–O1	2.311(9)	O1–Na1–O2	77.58(19)
Na1–O2	2.267(8)	C12–C11–C4–C5	114.7(11)
[Li(THF) $_2$] $_3$ [Eu(<i>S</i> -binol) $_3$], 4a			
Eu1–O1	2.277(11)	O1–Eu1–O3	82.8(3)
Eu1–O2	2.292(11)	O2–Eu1–O4	83.1(3)
Eu1–O3	2.306(12)	O5–Eu1–O6	82.6(3)
Eu1–O4	2.286(11)	O2–Li1–O1	94.6(11)
Eu1–O5	2.280(11)	O3–Li2–O6	96.1(12)
Eu1–O6	2.273(12)	O4–Li1–O5	96.9(10)
Li1–O1	1.88(3)	C1–C10–C11–C12	–117.0(14)
Li1–O2	1.86(2)	C21–C30–C31–C32	–108.8(14)
Li2–O3	1.83(3)	C41–C50–C51–C52	–112.1(14)
Li2–O6	1.83(2)		
Li3–O4	1.75(2)		
Li3–O5	1.88(2)		
[Li(THF) $_2$] $_3$ [Eu(<i>S</i> -binol) $_3$ (H $_2$ O)], 4b			
Eu2–O7	2.319(10)	O8–Eu2–O9	79.5(3)
Eu2–O8	2.326(10)	O10–Eu2–O11	77.9(3)
Eu2–O9	2.273(9)	O12–Eu2–O7	80.3(3)
Eu2–O10	2.339(11)	O7–Li4–O8	93.9(12)
Eu2–O11	2.373(12)	O9–Li5–O10	95.5(9)
Eu2–O12	2.307(11)	O11–Li6–O12	95.7(11)
Eu2–O13	2.616(10)	C61–C70–C71–C72	–116.3(13)
Li4–O7	1.85(3)	C101–C110–C111–C120	–110.4(14)
Li4–O8	1.81(2)	C81–C90–C91–C92	–112.3(14)
Li5–O9	1.81(2)		
Li5–O10	1.88(2)		
Li6–O11	1.86(2)		
Li6–O12	1.84(2)		
[Li(THF) $_2$] $_2$ [Li(Et $_2$ O)][Yb(<i>S</i> -binol) $_3$], 5			
Yb1–O1	2.199(10)	O1–Yb1–O2	82.6(3)
Yb1–O2	2.232(8)	O3–Yb1–O37	75.7(3)
Yb1–O3	2.193(9)	O2–Li1–O27	97.3(19)
Li1–O2	1.83(3)	O1–Li2–O3	86.6(10)
Li2–O1	1.98(3)	C10–C11–C21–C22	–120.8(16)
Li2–O3	1.96(3)	C30–C31–C317–C327	–116.5(11)
[Na(THF) $_2$] $_3$ [Yb(<i>R</i> -binol) $_3$], 6			
Yb1–O1	2.199(4)	O1–Yb1–O2	78.77(14)
Yb1–O2	2.226(4)	O1–Yb1–O25	81.72(15)
Na1–O1	2.390(5)	O1–Na1–O2	74.97(13)
Na1–O2	2.218(5)	C1–C10–C11–C12	120.3(6)

binaphthol to develop the synthetic route rather than the more expensive optically pure diol. The first complex we prepared was made by reaction of 3 equiv of *rac*-LiHbinol with [Y{N(SiMe $_3$) $_2$] $_3$, and we naively expected that the product would be a racemic mixture of *RRR*-Li $_3$ [Y(binol) $_3$] and its *SSS*-enantiomer. However the aromatic region of the ^{13}C NMR spectrum showed more than the 10 resonances that would be expected for this racemic mixture. The ^1H NMR spectrum was also very complex and showed a doublet at an unexpectedly high field (δ 5.82, J = 8.81 Hz), as shown in Figure 1. A single-crystal X-ray diffraction study of the complex

(7) Sasai, H.; Arai, T.; Satow, Y.; Houk, K. N.; Shibasaki, M. *J. Am. Chem. Soc.* **1995**, *117*, 6194–6198.

(8) Sasai, H.; Suzuki, T.; Itoh, N.; Tanaka, K.; Date, T.; Okamura, K.; Shibasaki, M. *J. Am. Chem. Soc.* **1993**, *115*, 10372–10373.

(9) Takaoka, E.; Yoshikawa, N.; Yamada, Y. M. A.; Sasai, H.; Shibasaki, M. *Heterocycles* **1997**, *46*, 157–163.

Table 2. Geometrical Data for $M_3[Ln(binol)_3]$ Complexes

compound	dihedral angles between naphthyl rings (deg)	M–M (Å)	O(T)–O(T) (Å)	O(B)–O(B) (Å)	deviation of Ln from M_3 plane (Å)
[Na(THF) ₂] ₃ [La(<i>S</i> -binol) ₃ (H ₂ O)], 7	65.8	6.080	4.059	3.456	0.488
[Li(Et ₂ O)] ₃ [Eu(<i>S</i> -binol) ₃], 4a	63.9	5.197	3.384	3.655	0.067
	64.0	5.402	3.557	3.711	
	67.0	5.291	3.427	3.545	
[Li(Et ₂ O)] ₃ [Eu(<i>S</i> -binol) ₃ (H ₂ O)], 4b	64.2	5.492	3.902	3.186	0.326
	67.0	5.048	3.660	3.235	
	65.6	5.141	4.100	3.520	
[Na(THF) ₂] ₃ [Eu(<i>S</i> -binol) ₃ (H ₂ O)] ^a	63.2	6.039	3.805	3.274	0.387
[Li(THF) ₂] ₃ [Y(<i>R</i> -binol) ₃], 1a^b	–63.0	5.471	3.506		0.000
	–63.0	5.471	3.468		
	–62.6	5.506	3.487		
[Na(THF) ₂] ₃ [Y(<i>R</i> -binol) ₃], 3	–56.2	5.947	3.531	3.256	0.372
[Li(THF) ₂] ₂ [Li(Et ₂ O)][Yb(<i>S</i> -binol) ₃], 5	58.0	5.229	3.300		0.000
	58.5	5.229	3.495		
		5.652	3.412		
[Na(THF) ₂] ₃ [Yb(<i>R</i> -binol) ₃], 6	60.0	5.926	3.231	3.500	0.330

^a Ref 8. ^b Ref 3.

showed it to be [Li(THF)₂]₃[Y(*R*-binol)₂(*S*-binol)], **2a**, and its *SSR*-enantiomer. The molecular structure of *RRS*-**2a** is shown in Figure 2. NMR studies have shown that this is the *only* complex formed and that it is stable in solution for prolonged periods: we have seen no ligand redistribution over a period of more than two years in *d*₈-THF solution in an NMR tube. Exclusive formation of *RRS*- and *SSR*-diastereomers was also observed on reaction of [Yb{N(SiMe₃)₂}₃] with *rac*-LiHbinol: the ¹H NMR spectrum of the paramagnetic product showed 17 well-separated resonances with chemical shifts from –32 to +84.4 ppm (see Table 3).

Formation of *SSR*-[W(binol)₃] (and presumably its *RRS* enantiomer) from reaction of WCl₆ with *rac*-H₂-binol has been reported by Hepert, but the structure has not been confirmed crystallographically.¹⁰ This complex was, however, formed as a statistical mixture with *SSS*- and *RRR*-[W(binol)₃], and so there appears to have been no strong directing force in this case. We have recently shown that *rac*-Li₂binol forms clusters of *SSR*- and *RRS*-[Li₆(binol)₃] both in the solid state and in solution, a self-assembly that appears to be directed by the coordination requirements of Li.¹¹

The exclusive formation of *RRS*- and *SSR*-[Li(THF)₂]₃-[Ln(binol)₃] indicates that there are significant differences compared with the [W(binol)₃] case. Comparison of the [Li(THF)₂]₃[Y(*R*-binol)₂] fragments of *RRR*- and *RRS*-[Li(THF)₂]₃[Y(binol)₃] does not highlight any gross structural differences, and so there does not seem to be any reason for the coordination preferences of Y to direct the formation of a *RRS*- rather than the *RRR*-diaste-

reomer. The solid state structure does, however, show a relatively close approach (2.881 Å) of H59 (the 3-position of the *S* binol) to C23 (the 4-position of the neighboring *R*-binol) as shown in Figure 3. It therefore seems possible that a weak C–H to π hydrogen-bond is responsible for the structural selectivity. “Edge-to face” attractive interactions have been recognized as important in directing supramolecular assembly of charged aromatic species,¹² and a detailed theoretical study of these interactions in benzene has been published.¹³ The large upfield shift observed for H3 of the unique binol ligand in the ¹H NMR spectrum of **2a** (δ 5.82 in *rac*-[Li(THF)₂]₃[Y(binol)₃] compared with δ 7.36 for the *RRR*-diastereomer) is not fully accounted for using the crystallographically determined coordinates for *RRS*-[Li(THF)₂]₃[Y(binol)₃],¹⁴ suggesting that in solution the edge-to-face interaction is somewhat closer and therefore stronger. A large upfield shift for the 3-proton of the unique binol in *SSR*-[W(binol)₃] has also been ascribed to an interaction with the π -system of the neighboring naphthyl ring.¹⁰

In contrast with our results using *rac*-LiHbinol, reaction of [Y{N(SiMe₃)₂}₃] with 3 equiv of *rac*-NaHbinol resulted in exclusive formation of *RRR*- and *SSS*-[Na(THF)₂]₃[Y(binol)₃], **3**. The molecular structure of *RRR*-**3** is shown in Figure 3. It is possible that the larger size of Na⁺ (four-coordinate radius = 113 pm) compared with Li⁺ (four-coordinate radius = 73 pm)¹⁵ prevents close edge-to-face approach of binol units of opposite chirality, and so formation of *RRS*- and *SSR*-diastereomers is not favored. Further evidence of the importance of

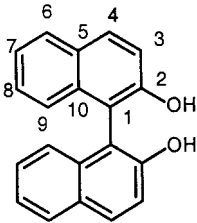
(10) Dietz, S. D.; Eilerts, N. W.; Heppert, J. A.; Morton, M. D. *Inorg. Chem.* **1993**, *32*, 1698–1705.

(11) Aspinall, H. C.; Bickley, J. F.; Dwyer, J. L. M.; Greeves, N.; Steiner, A. *Angew. Chem. Int. Ed.* **2000**, *39*, 2858–2861.

(12) Lindeman, S. V.; Kosynkin, D.; Kochi, J. K. *J. Am. Chem. Soc.* **1998**, *120*, 13268–13269.

(13) Jorgensen, W. L.; Severance, D. L. *J. Am. Chem. Soc.* **1990**, *112*, 4768–4774.

(14) Abraham, R. J.; Escruhuela, M. C. Personal communication.

Table 3. NMR Data for $M_3[Ln(binol)_3]$ Complexes^a


compound	¹ H	¹³ C
H ₂ binol ^b	7.15 d 9.0 9 , 7.31 ddd (8.5, 7, 1.5) 8 , 7.38 ddd (8.0, 7.0, 1.5) 7 , 7.39 d (9.0) 3 , 7.90 d (8.0) 6 , 7.98 d (8.0) 4	111.74 1 , 117.71 3 , 124.02 7 , 124.16 9 , 127.47 8 , 128.38 6 , 129.40 5 , 131.40 4 , 133.35 10 , 152.70 2
Li ₃ [La(binol) ₃]	6.90 m 6,7 , 6.99 m 8 , 7.15 d (8.68) 3 , 7.70 d (7.71) 9 , 7.715 d (9.16) 4	119.3, 120.5, 124.4, 124.9, 126.9, 128.2, 128.5, 136.9, 163.6
Na ₃ [La(binol) ₃]	6.82 6 , 6.83 7 , 6.90 8 , 7.37 d (9.12) 3 , 7.65 d (8.42) 9 , 7.72 d (9.13) 4	118.5, 119.9, 124.8, 126.2, 127.3, 128.0, 128.6, 136.5, 165.0
Li ₃ [Y(binol) ₃]	6.81 m 6,7 , 7.03 m 8 , 7.36 d (8.7) 3 , 7.74 d (7.9) 9 , 7.78 d (8.76) 4	120.31, 122.18 8 , 126.26 6 or 7 , 127.90 3 , 128.26 6 or 7 , 129.80 4,9 , 130.11, 137.61, 164.04 2
Na ₃ [Y(binol) ₃]	6.86 m 6,7 , 6.94 m 8 , 7.48 d (8.7) 3 , 7.67 d (8.7) 9 , 7.76 d (9.0) 4	116.8
<i>rac</i> -Li ₃ [Y(binol) ₃]	5.82 d (8.81), 6.7–8 complex pattern	118.9, 123.5, 124.58, 125.6, 126.8, 127.1, 134.4, 162.8, 117.5, 118.2, 118.9, 122.0, 122.9, 123.5, 124.2, 124.4, 125.4, 126.6, 126.8, 126.9, 127.2, 129.0, 134.6, 135.5, 158.6, 160.6
Li ₃ [Eu(binol) ₃]	3.04 br 9 , 6.07 br 8 , 8.13 br 7 , 8.73 vbr 6 , 9.33 br 4 , 12.32 br 3	116.77, 119.34, 122.61, 123.70, 129.59, 131.88
Li ₃ [Yb(binol) ₃]	−14.12 br 9 , −1.38 br 8 , 2.69 br 7 , 8.16 d (7.5) 6 , 24.00 br 4 , 90.35 br 3	59 br, 108.479, 111.120, 114.273, 116.431, 123 br, 123.974, 124.691, 139.5 br
Na ₃ [Yb(binol) ₃]	−2.24 d (8.59) 9 , 3.29 m 8 , 4.65 m 7 , 7.62 d (7.82) 6 , 14.73 s 4 , 44.41 s 3	98.1, 117.5 9 , 118.6 7 , 119.3 8 , 125.1, 125.4 6 , 127.0 3 , 133.1 4 , 149.8, 160
<i>rac</i> -Li ₃ [Yb(binol) ₃]	−32.08, −7.03, −6.87, 0.87, 2.95 (2H), 6.02, 6.30 d (8.0), 7.74 d (8.5), 8.34, 11.80, 11.91, 15.96, 17.19, 26.93, 46.33, 79.87, 84.42	
<i>rac</i> -Na ₃ [Yb(binol) ₃]	−4.33, 3.41, 4.80, 5.07, 5.15, 5.86, 6.09, 6.42 d (7.0), 6.80 m, 6.99 m, 7.46 m, 7.94, 8.76, 8.98, 13.26, 19.68, 25.82, 33.84	

^a All samples were dissolved in *d*₈-THF. Coupling constants (in Hz) are given in parentheses and assignments are given in **bold**. ^b Ref 18.

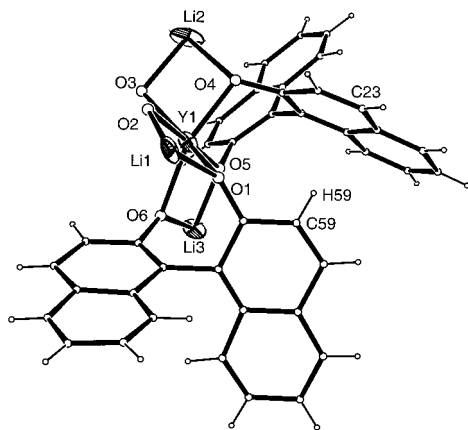


Figure 3. Close approach of H59 to C23 in [Li(THF)₂]₃[Y(*R*-binol)₂(*S*-binol)].

ionic size in determining the structures of $M_3[Ln(binol)_3]$ complexes is found in the reaction of $[Yb\{N(SiMe_3)_2\}_3]$ with *rac*-NaHbinol. In this case the product, characterized by ¹H NMR spectroscopy, is a mixture of *RRR*-/*SSS*- and *RRS*-/*SSR*-Na₃[Yb(binol)₃] in the ratio of ca. 3:1.

Molecular mechanics calculations (CACH 4.1.1 using augmented MM2 parameters) have failed to shed any light on the observed structural selectivity in formation of *rac*- $M_3[Ln(binol)_3]$ complexes. The gross structural

features of *RRR*-[Li(THF)₂]₃[Y(binol)₃] can be reproduced reasonably successfully (although calculated dihedral angles for the binol ligands are ca. 12° larger than those observed), but this is not the case for *RRS*-[Li(THF)₂]₃[Y(binol)₃]. This indicates that the formation of *RRS*- $M_3[Ln(binol)_3]$ is governed by more subtle effects than simple steric preferences.

RRS- and *SSR*-[Li(THF)₂]₃[Ln(binol)₃] are a new type of chiral $M_3[Ln(binol)_3]$ complex. Their ready formation suggests that enantioselective catalysts and reagents should be available from binaphthol of low optical purity, leading to nonlinear effects in enantioselective reactions.¹⁶ A positive nonlinear effect has already been observed in the nitroaldol reaction catalyzed by lithium–lanthanum–binaphtholate.¹⁷

X-ray Diffraction Studies. We have determined the crystal structures of $M_3[Ln(binol)_3]$ for the following compounds: Ln = Eu, M = Li, **4**; Ln = Y, M = Li or Na, **3**; and for Ln = Yb, M = Li, **5**, or Na, **6**. Selected bond distances and angles are given in Table 1. In our work on enantioselective alkylation of aldehydes, the best ee's were obtained for Ln = La, and so we were particularly interested in the structures of $M_3[Ln(binol)_3]$ where Ln is an early lanthanide. However, crystals of [Li(THF)₂]₃[La(binol)₃] always broke down to

(16) Girard, C.; Kagan, H. B. *Angew. Chem., Int. Ed. Engl.* **1998**, *37*, 2923–2959.

(17) Sasai, H.; Suzuki, T.; Itoh, N.; Shibasaki, M. *Tetrahedron Lett.* **1993**, *34*, 851–854.

(15) Shannon, R. D. *Acta Crystallogr.* **1976**, *A32*, 751.

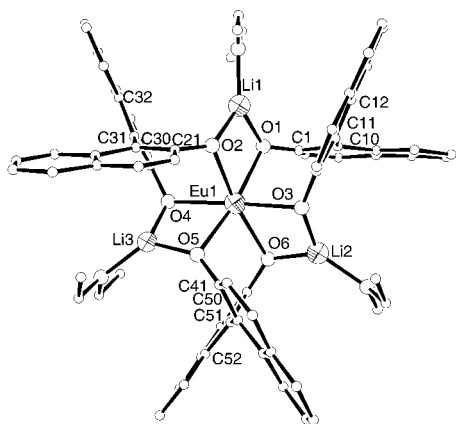


Figure 4. Molecular structure of $[\text{Li}(\text{OEt}_2)_3][\text{Eu}(\text{S-binol})_3]$, **4a**.

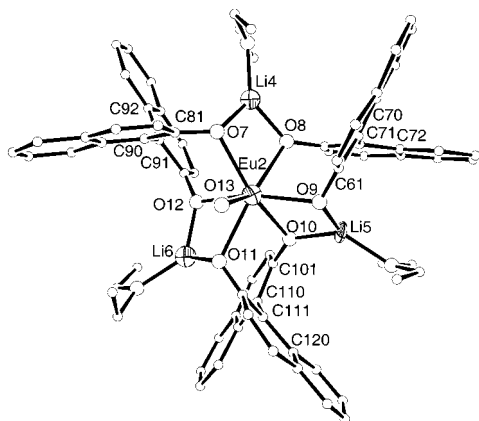


Figure 5. Molecular structure of $[\text{Li}(\text{OEt}_2)_3][\text{Eu}(\text{S-binol})_3(\text{H}_2\text{O})]$, **4b**.

an amorphous powder in the absence of mother liquor, and so we were unable to determine the solid state structure of this complex. Similar problems were encountered with other large lanthanides Pr and Ce. The crystals that eventually grew from a THF solution of $\text{Na}_3[\text{La}(\text{binol})_3]$ were found to be $[\text{Na}(\text{THF})_2]_3[\text{La}(\text{binol})_3(\text{H}_2\text{O})]$, **7**. The structure of **7** has already been reported by Shibasaki, but the coordinates and details of structure determination were not published in full.⁷ Eu is the largest Ln for which we have been able to obtain good quality crystals of $\text{Li}_3[\text{Ln}(\text{binol})_3]$. In this case crystals were grown from Et_2O solution. Crystal growth was very slow (several weeks), and X-ray diffraction showed the crystal to be made up of one molecule of $[\text{Li}(\text{OEt}_2)_3][\text{Eu}(\text{binol})_3]$, **4a**, and one molecule of $[\text{Li}(\text{OEt}_2)_3][\text{Eu}(\text{binol})_3(\text{H}_2\text{O})]$, **4b**. The structures of these complexes are shown in Figures 4 and 5, respectively. The presence of one molecule of the aquo complex and one molecule of the anhydrous complex in these stable crystals accounts for the reluctance of this complex to crystallize: ingress of sufficient atmospheric moisture into the Schlenk tube to form this mixture is expected to be a slow process. Nevertheless, this allows direct comparison of anhydrous and aquo complexes. The most pronounced difference between **4a** and **4b** is the greater pyramidalization of the Li_3Eu fragment in the aquo complex. The Eu atom is 0.326 Å out of the Li_3 plane in the aquo complex **4b** compared with only 0.067 Å in the anhydrous complex **4a**. The corresponding deviation from the M_3 plane in $[\text{Na}(\text{THF})_2]_3[\text{Eu}(\text{binol})_3(\text{H}_2\text{O})]$ is

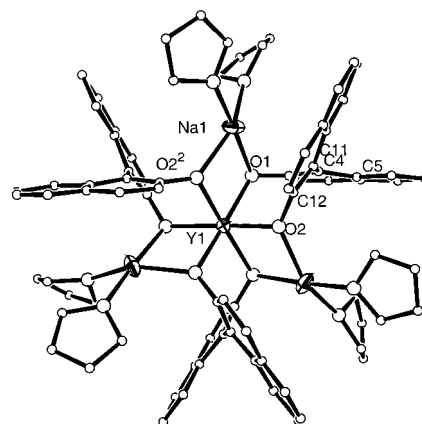


Figure 6. Molecular structure of $\text{SSS-}[\text{Na}(\text{THF})_2]_3\text{-}[\text{Y}(\text{binol})_3]$, **3**. O2 and O22 are related by a C_3 rotation through Y1.

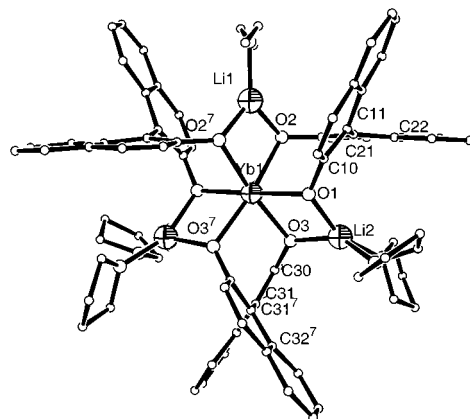


Figure 7. Molecular structure of $[\text{Li}(\text{THF})_2]_2[\text{Li}(\text{Et}_2\text{O})][\text{Yb}(\text{S-binol})_3]$, **5**. O3 and O37, and C31 and C37 are related by a C_2 rotation about Li1–Yb1.

0.387 Å. The effect of this pyramidalization is to close up the binding site at Ln on the face opposite the neutral donor and thus to modify the way in which a substrate molecule interacts with the chiral ligand environment.

The crystal structure of $[\text{Li}(\text{THF})_3][\text{Y}(\text{R-binol})_3]$, **1a**, has already been published. In the present work we have characterized crystallographically *RRR*- and *SSS*- $[\text{Na}(\text{THF})_2]_3[\text{Y}(\text{binol})_3]$, **3**, as well as the Yb complexes $[\text{Li}(\text{THF})_2]_2[\text{Li}(\text{Et}_2\text{O})][\text{Yb}(\text{S-binol})_3]$, **5**, and $[\text{Na}(\text{THF})_2]_3\text{-}[\text{Yb}(\text{S-binol})_3]$, **6**. **5** crystallizes in the rare space group $P6_5_{22}$, of which the Cambridge Crystallographic Data Base has only 21 examples out of a total of 215 000 entries. The molecular structures of **3**, **5**, and **6**, along with selected geometrical data are shown in Figures 6, 7, and 8, respectively. Some comparative geometrical data for $\text{M}_3[\text{Ln}(\text{binol})_3]$ complexes are summarized in Table 2. The absolute values of the dihedral angles between naphthyl rings of the binol ligands vary from 56.2° ($[\text{Na}(\text{THF})_2]_3[\text{Y}(\text{binol})_3]$) to 67° ($[\text{Li}(\text{OEt}_2)_3][\text{Eu}(\text{binol})_3(\text{H}_2\text{O})]$), illustrating how the flexible binol fragment can accommodate a wide range of coordination requirements. For the $\text{Li}_3[\text{Ln}(\text{binol})_3]$ complexes there is a general decrease in binol dihedral angle on traversing the Ln series from Eu to Yb. Perhaps the most striking feature of the structures is the deviation of Ln from the M_3 plane. When $\text{M} = \text{Na}$, this deviation is always significant, even though the complexes are anhydrous, and there is thus no neutral-ligand-induced

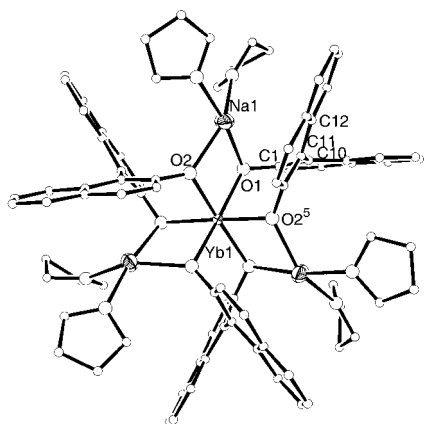


Figure 8. Molecular structure of $[\text{Na}(\text{THF})_2]_3[\text{Yb}(\text{S-binol})_3]$, **6**. O2 and O25 are related by a C_3 rotation through Yb1.

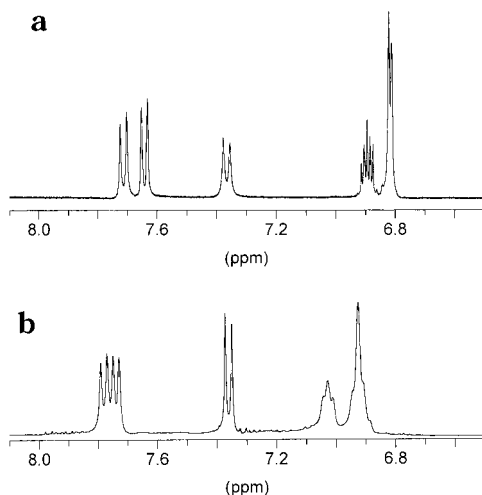


Figure 9. ^1H NMR spectra (aromatic region) of $\text{Li}_3[\text{Ln}(\text{binol})_3]$ (a) $\text{Ln} = \text{La}$ (b) $\text{Ln} = \text{Y}$.

pyramidalization. When $M = \text{Li}$, the $M_3\text{Ln}$ fragment is close to planar (as in $[\text{Li}(\text{OEt})_2]_3[\text{Eu}(\text{binol})_3]$) or has crystallographically imposed planarity (as in $[\text{Li}(\text{THF})_2]_3[\text{Y}(\text{binol})_3]$ and $[\text{Li}(\text{THF})_2]_2[\text{Li}(\text{OEt})_2][\text{Yb}(\text{binol})_3]$). NMR studies (see discussion below) show that all of the anhydrous complexes have D_3 symmetry in solution between room temperature and 173 K. Although it is not at all surprising that some of the complexes have lower symmetry in the solid state than in solution, it is not immediately clear why the Na-containing complexes adopt a pyramidal structure in the solid state and the Li-containing complexes do not.

NMR Studies. NMR data (^1H and ^{13}C) are summarized in Table 3, along with the published data for H_2binol .¹⁸ Assignments were made by two-dimensional spectroscopy (COSY and HXCO). All of the *RRR*- or *SSS*-complexes that we have investigated have D_3 symmetry in solution: they have six inequivalent aromatic protons and 10 inequivalent C atoms. We have found that the aromatic regions of the ^1H NMR spectra of the diamagnetic complexes are sensitive to the identities of Ln and of M, as illustrated in Figure 9a,b. These differences appear to be related to the dihedral angle between the two naphthyl rings of a binol ligand

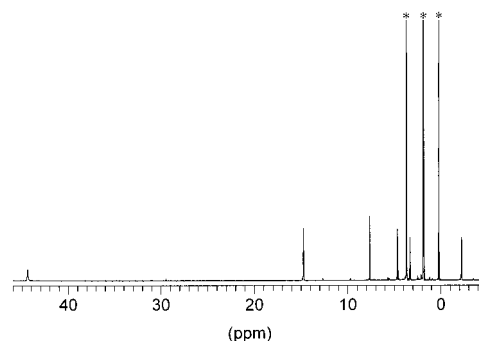


Figure 10. ^1H NMR spectrum of $\text{Na}_3[\text{Yb}(\text{S-binol})_3]$. Resonances marked * are due to solvent and TMS.

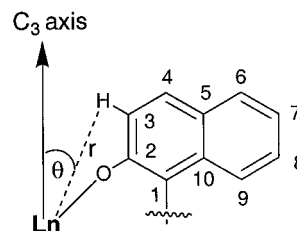


Figure 11. Diagram to illustrate the geometrical parameters used in the analysis of NMR spectra of paramagnetic complexes.

and the associated ring-current effects. The protons of each binol ligand are also affected by ring-currents in the neighboring binols;¹⁴ a detailed investigation will form the subject of a separate paper.

The high-symmetry $M_3[\text{Ln}(\text{binol})_3]$ complexes provide a rare opportunity to make a straightforward investigation of the dipolar contribution to the chemical shifts of paramagnetic complexes containing Yb^{3+} ($4f^{13}$) and Eu^{3+} ($4f^6$). The aromatic ^1H resonances of $M_3[\text{Yb}(\text{binol})_3]$ cover a remarkably wide range of +90 to −14.12 ppm for $M = \text{Li}$ and +44 to −2.24 ppm for $M = \text{Na}$. The ^1H NMR spectrum of $[\text{Na}(\text{THF})_2]_3[\text{Yb}(\text{S-binol})_3]$ in d_8 -THF is shown in Figure 10. The geometrical factor $(3 \cos^2 \theta - 1)/r^3$, defined in Figure 11, was calculated for each aromatic proton using average values from crystallographic data. The induced shift $\Delta\delta$ was calculated by comparison with the spectrum of the diamagnetic complex $[\text{Na}(\text{THF})_2]_3[\text{Y}(\text{binol})_3]$.

Plots of $\Delta\delta$ against $(3 \cos^2 \theta - 1)/r^3$ for $\text{Na}_3[\text{Yb}(\text{binol})_3]$ and $\text{Li}_3[\text{Yb}(\text{binol})_3]$ give straight lines, as shown in Figure 12, showing that the paramagnetic shift is entirely dipolar in origin and that there is no delocalization of the unpaired electron of Yb onto the protons of the aromatic rings. The difference in gradient between the lines for $M = \text{Na}$ and $M = \text{Li}$ indicates a difference in the crystal field parameters for the two complexes. ^{13}C NMR chemical shifts do not show a simple linear dependence on geometrical factor, indicating that there is some contact contribution to the induced shift of the aromatic C atoms. The complexes retain D_3 symmetry in solution down to 173 K: variable-temperature ^1H NMR spectra of $\text{Na}_3[\text{Yb}(\text{binol})_3]$ (298–173 K) show a linear dependence of shift on $1/T^2$, proving that there is no structural change in this temperature range. The large chemical shift range observed for the aromatic protons of the paramagnetic $M_3[\text{Ln}(\text{binol})_3]$ and their great sensitivity to geometrical change suggest that NMR spectroscopy of paramagnetic

(18) Yashima, E.; Yamamoto, C.; Okamoto, Y. *J. Am. Chem. Soc.* **1996**, *118*, 4036–4048.

Table 4. Experimental Details for X-ray Structure Determination

	<i>rac</i> -[Li(THF) ₂] ₃ - [Y(binol) ₃] ₃ ·THF, 2a	<i>rac</i> -[Na(THF) ₂] ₃ - [Y(binol) ₃], 3	[Li(OEt ₂) ₃ Eu(binol) ₃] [Li(OEt ₂) ₃ Eu(binol) ₃ (H ₂ O)]· 2Et ₂ O, 4	[Li(THF) ₂] ₂ [Li(OEt ₂)]- [Yb(binol) ₃] ₃ · THF, 5	[Na(THF) ₂] ₃ - [Yb(binol) ₃], 6	[Na(THF) ₂] ₃ [La(binol) ₃ - (H ₂ O)], 7
empirical formula	C ₈₈ H ₉₂ Li ₃ O ₁₃ Y	C ₈₄ H ₈₄ Na ₃ O ₁₂ Y	C ₇₆ H _{75.50} EuLi ₃ O _{10.50}	C ₈₈ H ₉₄ Li ₃ O ₁₃ Yb	C ₈₄ H ₈₄ Na ₃ O ₁₂ Yb	C ₈₄ H ₈₆ LaNa ₃ O ₁₃
fw	1467.53	1443.56	1329.79	1553.68	1527.69	1511.49
space group	<i>P</i> 1	<i>R</i> 3 <i>c</i>	<i>P</i> 2 ₁	<i>P</i> 6 ₅₂₂	<i>P</i> 6 ₃	<i>P</i> 6 ₃
<i>a</i> (Å)	15.645(3)	15.1989(16)	14.9654(16)	15.1157(10)	15.1044(17)	15.2581(17)
<i>b</i> (Å)	16.760(4)	15.1989(16)	37.174(3)	15.1157(10)	15.1044(17)	15.2581(17)
<i>c</i> (Å)	19.187(6)	55.338(9)	15.1520(15)	59.098(7)	18.419(2)	18.207(2)
α (deg)	111.34(3)	90.00	90.00	90.00	90.00	90.00
β (deg)	103.23(3)	90.00	118.496(12)	90.00	90.00	90.00
γ (deg)	96.79(3)	120.00	90.00	120.00	120.00	120.00
<i>V</i> (Å ³)	4447.7(19)	11071(2)	7408.3(12)	11693.9(17)	3639.2(7)	3670.8(7)
<i>Z</i>	2	6	4	6	2	2
<i>D</i> _{calc} (g/cm ³)	1.096	1.299	1.192	1.324	1.394	1.366
<i>F</i> (000)	1544	4535	2750	4829	1574	1564
μ (Mo Kα) (mm ⁻¹)	0.674	0.826	0.830	1.181	1.279	0.595
θ range (deg)	1.99 < θ < 22.49	1.71 < θ < 22.48	1.53 < θ < 22.45	1.56 < θ < 22.49	1.91 < θ < 22.48	1.90 < θ < 22.99
index range	-16 ≤ <i>h</i> ≤ 16 -18 ≤ <i>k</i> ≤ 17 -20 ≤ <i>l</i> ≤ 20	-16 ≤ <i>h</i> ≤ 16 -16 ≤ <i>k</i> ≤ 16 -59 ≤ <i>l</i> ≤ 59	-16 ≤ <i>h</i> ≤ 16 -37 ≤ <i>k</i> ≤ 39 -16 ≤ <i>l</i> ≤ 16	-16 ≤ <i>h</i> ≤ 16 -16 ≤ <i>k</i> ≤ 13 -59 ≤ <i>l</i> ≤ 63	-16 ≤ <i>h</i> ≤ 16 -16 ≤ <i>k</i> ≤ 16 -19 ≤ <i>l</i> ≤ 19	-16 ≤ <i>h</i> ≤ 16 -16 ≤ <i>k</i> ≤ 16 -19 ≤ <i>l</i> ≤ 19
no. of reflns collected	20 202	19 853	31 624	45 247	19 569	21 050
no. of unique reflns	10 951	3211	17 310	5072	3144	3400
no. of reflns (<i>I</i> > 2σ(<i>I</i>))	1593	1812	10151	4266	2786	2785
R1 (<i>I</i> > 2σ(<i>I</i>))	0.0837	0.0596	0.0648	0.0986	0.0269	0.0250
wR2 (all data)	0.2174	0.1227	0.1685	0.2263	0.0645	0.0545
absolute structure param			0.020(16)	-0.033(30)	0.023(14)	-0.03(2)
no. of data/params/ restraints	10 951/941/1000	3211/294/162	17310/1445/501	5072/389/160	3144/295/11	3400/304/69
GOF on <i>F</i> ²	0.589	0.841	0.826	1.043	1.098	0.933

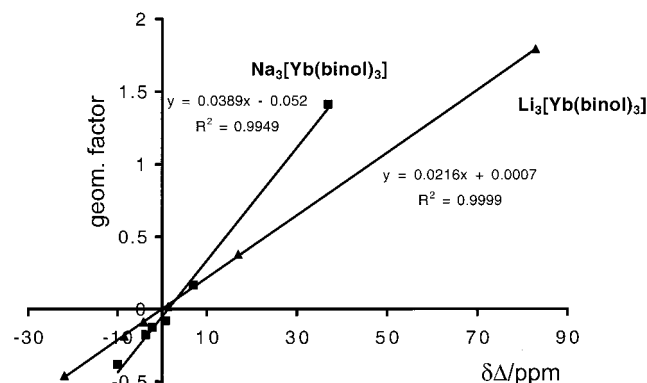


Figure 12. Plots of $\Delta\delta$ against geometrical factor $10^3 \times (3 \cos^2 \theta - 1)/r^3$ for $M_3[Yb(binol)_3]$ ($M = Li$ or Na).

species should be an excellent technique for studying the detailed coordination chemistry of these complexes.

Conclusions

We have determined the crystal structures of a range of $M_3[Ln(binol)_3]$ complexes which have been shown to be excellent catalysts and reagents for enantioselective synthesis, and the binol ligand has again been shown to accommodate a range of metal radii. 1H NMR spectra of aromatic protons have been found to be highly sensitive to the dihedral angles between naphthyl rings, and NMR spectroscopy of paramagnetic complexes appears to be a promising technique for detailed investigation of coordination chemistry in solution. A remarkable selectivity for formation of *RRS*- $M_3[Ln(binol)_3]$ and its *SSR*-enantiomer from *rac*-MHbinol has been found when $M = Li$, but not when $M = Na$, possibly opening the way for the preparation of chiral catalysts and reagents from binaphthol of low optical purity.

Experimental Section

Unless otherwise stated, all the preparations described below were performed under strictly anaerobic conditions using standard Schlenk techniques. Solvents were distilled from sodium/benzophenone ketyl (nondeuterated) or CaH_2 (deuterated) and stored under N_2 over 4 Å molecular sieves prior to use. Samples for NMR spectroscopy were sealed under vacuum, and spectra were recorded on a Gemini 300 or a Bruker AMX400 spectrometer. Elemental analyses were performed in duplicate by Mr. S. Apter of this Department.

Preparation of $[M]_3[Ln(binol)_3]$. The preparation of all the $[M]_3[Ln(binol)_3]$ complexes was carried out in a similar

manner. As a typical example the preparation of $[Li(THF)_2]_3[Y(R-binol)_3]$ is described: $Li[R-binol]$ was prepared by addition of Bu^oLi in hexane (1 equiv) to a solution of *R*-H₂-binol (0.794 g, 2.77 mmol) in THF (10 cm³) at 0 °C. To this solution was added a solution of $[Y\{N(SiMe_3)_2\}_3]$ (0.526 g, 0.923 mmol) in Et₂O (15 cm³). The reaction mixture was stirred at 0 °C until a clear solution had formed (ca. 10 min). Solvent was then removed in vacuo, and the resulting white solid was recrystallized from THF–petroleum ether at –20 °C to give product as colorless prisms. Yield = 0.741 g (57.5%). Preparation of Na/Ln complexes used $Na[Hbinol]$ prepared from Hbinol and NaH in THF solution. Preparation of *rac* complexes used *rac*- $M[Hbinol]$ ($M = Li$ or Na) instead of optically pure $M[Hbinol]$.

Anal. *rac*- $[Li(THF)_2]_3[Y(binol)_3] \cdot THF$: $C_{88}H_{92}Li_3O_{13}Y$ 2 requires C, 72.03; H, 6.32. Found: C, 70.37; H, 5.93. $[Li(THF)_2]_3[La(binol)_3]$: $C_{84}H_{84}LaLi_3O_{12}$ requires C, 69.81; H, 5.86. Found: C, 69.24; H, 6.22. *rac*- $[Li(THF)_2]_3[La(binol)_3]$: $C_{84}H_{84}LaLi_3O_{12}$ requires C, 69.81; H, 5.86. Found: C, 67.75; H, 6.00. $[Li(THF)_2]_3[Pr(binol)_3]$: $C_{84}H_{84}Li_3O_{12}Pr$ requires C, 69.71; H, 5.85. Found: C, 66.46; H, 5.43. $[Li(THF)_2]_3[Eu(binol)_3]$: $C_{84}H_{84}EuLi_3O_{12}$ requires C, 69.18; H, 5.81. Found: C, 63.52; H, 5.61. $[Li(THF)_2]_2[Li(OEt)] [Yb(S-binol)_3]$ (X-ray crystals): $C_{80}H_{78}Li_3O_{11}Yb$ requires C, 68.18; H, 5.58. Found: C, 66.22; H, 5.93. $[Na(THF)_2]_3[Y(R-binol)_3]$: $C_{84}H_{84}Na_3O_{12}Y$ requires C, 67.56; H, 5.54. Found: C, 65.42; H, 5.52. *rac*- $[Na(THF)_2]_3[Y(binol)_3]$: $C_{84}H_{84}Na_3O_{12}Y$ requires C, 67.56; H, 5.54. Found: C, 68.71; H, 5.84. $[Na(THF)_2]_3[Yb(S-binol)_3]$: $C_{84}H_{84}Na_3O_{12}Yb$ requires C, 66.04; H, 5.54. Found: C, 64.12; H, 5.43. *rac*- $[Na(THF)_2]_3[Yb(binol)_3]$: $C_{84}H_{84}Na_3O_{12}Yb$ requires C, 66.04; H, 5.54. Found: C, 65.80; H, 5.52. *rac*- $[Li(THF)_2]_3[Yb(binol)_3]$: $C_{84}H_{84}Li_3O_{12}Yb$ requires C, 70.72; H, 5.93. Found: C, 70.22; H, 5.84.

X-ray Crystal Structure Determinations. All X-ray data were collected at 213(2) K using a STOE-IPDS image plate diffractometer (Mo K α , graphite monochromator) in the φ rotation scan mode. The structures were solved by direct methods with the SHELXS97 package and refined using full-matrix least-squares on F^2 (SHELXL97). Absolute structures of **4**, **5**, **6**, and **7** were determined from the values of the Flack parameter. Experimental data for the individual structure determinations are summarized in Table 4.

Acknowledgment. We are grateful to EPSRC for financial support (studentships to J.L.M.D. and R.V.K.) and to Rhodia Rare Earths for a gift of rare earth oxides.

Supporting Information Available: A listing of atomic coordinates, thermal parameters, bond lengths and angles, and atom numbering schemes for compounds **2**, **3**, **4**, **5**, **6**, and **7**. This material is available free of charge via the Internet at <http://pubs.acs.org>.

OM0006256